

Plasmonic implementation of a quantum eraser for imaging applications

J. Ajimo,¹ M. Marchante,¹ A. Krishnan,^{2,3} A. A. Bernussi,^{2,3} and L. Grave de Peralta^{1,3,a)}

¹Department of Physics, Texas Tech University, Lubbock, Texas 79409, USA

²Department of Electrical and Computer Engineering, Texas Tech University, Lubbock, Texas 79409, USA

³Nano Tech Center, Texas Tech University, Lubbock, Texas 79409, USA

(Received 13 April 2010; accepted 3 August 2010; published online 27 September 2010)

We describe the use of a plasmonic version of a quantum eraser for imaging applications. Two perpendicular surface plasmon polariton (SPP) beams were excited in a glass-metal sample using a leakage radiation microscope. The polarization state of the SPP-coupled radiation leaked to the sample substrate permits to identify the path of photons along the metal-air interface of the sample. Introduction of a linear polarizer after the microscope high numerical aperture lens erases the which-path information. This enabled us to image on the microscope charge coupled device camera the interference pattern formed in the sample surface. © 2010 American Institute of Physics.

[doi:10.1063/1.3485810]

I. INTRODUCTION

The pursuit of knowledge concerning the fundamentals of quantum mechanics has largely motivated the interest on quantum erasers.¹⁻³ Experiments with quantum erasers helped to establish that which-path information and visibility of interference fringes are complementary quantities: any distinguishability between the paths of interfering beams of light destroys the quality (visibility) of the interference fringes.³ In the simplest quantum eraser,⁴ diffraction of light by a double-slit experiment with a vertical polaroid placed before one slit and a horizontal polaroid before the other one did not display interference fringes because the path through each slit is labeled by orthogonal states of polarization. The which-path information may be removed and the interference restored by placing a polaroid oriented at 45° angle with respect to the vertical direction somewhere between the two-slit screen and the detection screen.

In this work, we describe a quantum eraser for non-disturbing imaging the interference pattern formed when two perpendicular surface plasmon polariton (SPP) beams cross each other. We implemented the quantum eraser using a leakage radiation microscope (LRM). In order to excite SPPs that propagate in the metal-air interface of a fabricated sample, the excitation light was focused in scattering features patterned in the sample surface using a low numerical aperture objective lens.^{5,6} Collection of the SPP-coupled radiation that leaks to the sample glass substrate during the propagation of SPPs along the metal-air interface was done using an immersion oil objective lens with high numerical aperture.⁵⁻⁸ Leakage radiation microscopy is an ideal technique to study the propagation of SPPs because the photons used for imaging are the ones that regardless of the measurement process leak into the sample substrate. This can be advantageously used for non-disturbing observation of SPP propagation. In alternative state of the art methods for imaging SPP propagation, such as near-field scanning optical microscopes,⁹ an optical tip is often placed in close proximity to the region to be

imaged, which introduces unavoidable perturbations in the original distribution of electromagnetic fields in the sample. We show here that in order to achieve the full potential of LRMs, one has to be able to introduce a which-path eraser (linear polarizer) in the optical path of the leakage radiation. We demonstrate the potential of this technique by using a LRM-based quantum eraser for non-disturbing observation of the two-dimensional interference pattern formed in the metal-air interface of a fabricated sample.

II. EXPERIMENTS AND DISCUSSION

Figure 1 shows schematic illustrations of the SPP collection [Fig. 1(a)] and excitation [Fig. 1(b)] techniques used in this work. Details of the LRM collection technique used here have been previously reported.^{10,11} As illustrated in Fig. 1(a), after excitation of SPP at the sample surface, radiation leaked to the sample substrate is collected by a 100× immersion oil

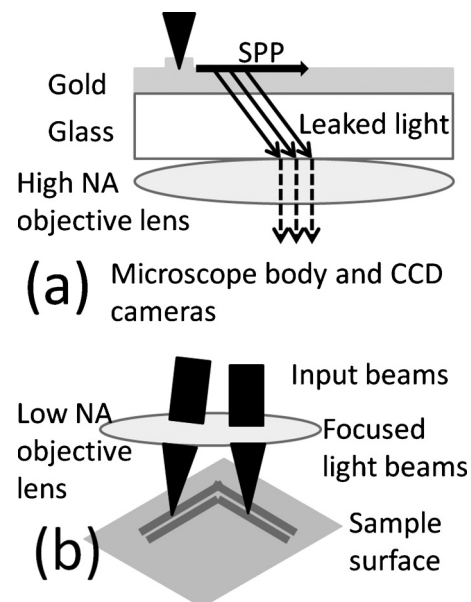


FIG. 1. Schematic illustrations of (a) SPP collection and (b) excitation techniques used in this work.

^{a)}Electronic mail: luis.grave-de-peralta@ttu.edu.

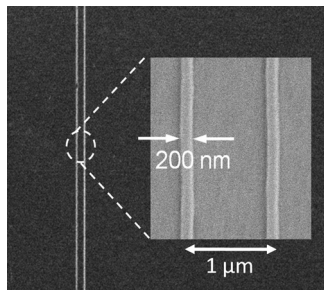


FIG. 2. SEM image of a fragment of the double-stripe structure forming each side of the \perp shape structure patterned on the sample surface. As shown in the inset, the width of the double-stripe structure is of $\sim 1 \mu\text{m}$. Each stripe corresponds to a gold ridge of 200 nm width.

objective lens with high numerical aperture ($\text{NA}=1.3$). A set of three lenses (not shown), internal to the microscope body, perform magnification and image formation. A charge coupled device (CCD) camera captures the image of the sample surface emission.^{10,11} In addition, a linear polarizer (which-path eraser) can be introduced after the immersion oil objective lens. In this work, we used the standard SPP excitation technique in LRM.^{5,6} As illustrated in Fig. 1(b), the excitation light is focused in scattering features patterned on the sample surface using a low numerical aperture objective lens ($\text{NA}=0.65$, $40\times$). Samples investigated here were patterned on a glass substrate. A 50 nm thick gold layer was initially deposited on top of a 1 nm thick chromium adhesion layer. The gold layer was covered with poly(methyl methacrylate) (PMMA) as the resist for the e-beam patterning. A pattern, forming a corner of a square (\perp shape), was defined onto the PMMA layer by e-beam lithography. After developing the PMMA, a second 50 nm thick layer of gold was deposited on the top of the PMMA layer. A final lift-off step produced the desired pattern with \perp shape. As illustrated in Fig. 1(b), each side of the \perp pattern consists of a $100 \mu\text{m}$ long double-stripe structure. Figure 2 shows a scanning electron microscopy (SEM) image of a fragment of the double-stripe structure forming each side of the \perp shape structure patterned on the sample surface. As shown in the inset, the width of the double-stripe structure is of $\sim 1 \mu\text{m}$. Each stripe corresponds to a gold ridge of 200 nm width. The patterned \perp -shape structure was used to launch two SPP beams perpendicular to each other on the 50 nm thick gold film. The excitation source was provided by a 10 mW He-Ne laser that emits linearly polarized light. The laser beam was equally divided by a 50/50 cube beam splitter. As illustrated in Fig. 1(b), the two beams were deflected toward the low numerical aperture microscope objective lens with slightly different angles. The lens focused the beams into spots $\sim 5 \mu\text{m}$ in diameter on each side of the \perp pattern. The beams were focused between the ridges of the double-stripe structure. This increases the SPP coupling efficiency of the excitation light in comparison with the use of a single ridge as the scattering feature. This procedure was used to excite two SPP beams that propagate on the gold-air interface perpendicularly to each side of the \perp pattern.^{5,6} In order to erase from the images two of the four launched SPP beams, an adequate spatial filter was introduced at the back focal plane (BFP) of the immersion oil objective lens.⁸

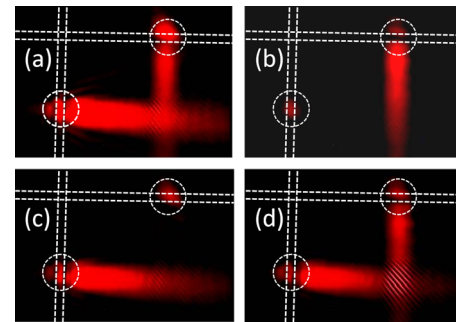


FIG. 3. (Color online) LRM images of the sample surface emission obtained (a) without and [(b)–(d)] with a linear polarizer introduced after the oil immersion objective. Images were taken with the transmission axis of the polarizer forming an angle of (b) 0° , (c) 90° , and (d) 45° with the polarization direction of the radiation leaked along the SPP beam seen vertical in the figures. Dashed circles, drawn at scale, have a diameter of $\sim 5 \mu\text{m}$. They illustrate the position of the focused spots. Added discontinuous lines (not at scale) correspond to the \perp pattern used for launching the SPP beams.

Figure 3 shows images of the sample surface emission taken with the LRM. In order to facilitate visual comparison, all the images were taken in the same conditions and displayed with the same saturation. The \perp shape patterned on the sample surface is also illustrated in Fig. 3 as dashed white lines. The sample surface emission image shown in Fig. 3(a) was obtained without adding a polarizer in the optical path of the leakage radiation. Two perpendicular SPP beams crossing each other are clearly seen. The image is formed on the microscope CCD camera by the SPP-coupled radiation that leaks from any point of the sample metal-air interface that the SPP excitation passes through. Regardless the polarization direction of the linearly polarized light emitted by the laser source, only the fraction of the input light that is scattered with TM polarization (by the \perp shape structure patterned on the sample surface) can excite SPPs.¹² Consequently, as long as the two SPP beams are excited simultaneously in the metal-air interface of the sample, we expect to observe clear interference fringes in the region where the two SPP beams cross each other. However, this is hardly the case in Fig. 3(a). The absence of clear interference fringes in Fig. 3(a) is due to the different states of polarization of the leakage radiation. The direction of the electric field of the light that leaks along one of the SPP beams is perpendicular to the direction of the electric field of the light that leaks along the other beam.^{13–15} This well known property was verified by introducing a linear polarizer after the BFP of the immersion oil objective lens.¹⁰ As shown in Figs. 3(b) and 3(c), the insertion of a linear polarizer, with the transmission axis parallel to the polarization direction of the light leaked along the direction of propagation of one of the beams, results in the erasure of the another beam from the surface emission image. Thus, the polarization state of the photons arriving at the CCD camera can be used for identifying the path followed by the leaked photons. This smear out the interference fringes actually existing at the metal-air interface of the sample from the image of it formed at the CCD camera [see Fig. 3(a)]. The intensity profile along the center of each SPP beam was measured and fitted to an exponential decay curve (not shown) to determine the SPP propagation

length in the sample.⁵ We determined a propagation length of $\sim 11 \mu\text{m}$ in good correspondence with reported values of $\sim 10 \mu\text{m}$ for thin gold films in the visible range.^{12,16} In addition, we performed a two-dimensional finite element simulation of SPP propagation.¹⁷ In good correspondence with the experimentally determined value, a propagation length of $9.3 \mu\text{m}$ was obtained from the simulation. A total observable propagation length of $\sim 25 \mu\text{m}$ was verified in our experiments (see Fig. 3).

In order to erase the which-path information, we rotated the transmission axis of the linear polarizer 45° angle with respect to the polarization directions of the leakage radiation. After removing the which-path information with the polarizer, as shown in Fig. 3(d), well-defined interference fringes are observed in the region of the sample surface emission image where the two beams cross each other. The separation between consecutive interference maxima in the direction of propagation of the beams is equal to the SPP wavelength, λ_{SPP} .¹⁸ We obtained in this way a SPP wavelength value of $\lambda_{\text{SPP}} \sim 614 \text{ nm}$. Using this value of λ_{SPP} and the following expressions:¹²

$$\lambda_{\text{SPP}} = \frac{\lambda_0}{n_s \sin(\theta_{\text{SPP}})}$$

with $\lambda_0 = 632.8 \text{ nm}$, and a substrate refractive index value of $n_s = 1.515$; we calculated $\theta_{\text{SPP}} \sim 42.9^\circ$ for the SPP excitation angle in a Kretschmann configuration, which is in good correspondence with the value of 44.5° reported in the literature.^{12,19} It is worth noting that the interference maxima shown in Fig. 3(d) are so intense that it partially saturates the CCD camera. This in contrast with the almost imperceptible fringes observed in Figs. 3(a) and 3(c). We explain the presence of this poorly defined pattern as a result of the interference of the leakage radiation with a small fraction of the direct light of the input laser beam that traversed the gold layer without coupling to SPPs and arrived to the CCD camera. The observation of the weak fringes in Fig. 3(c) and not in Fig. 3(b) suggests that the polarization state of the residual direct light was equal to the leaked SPP-coupled light producing the image shown in Fig. 3(c) and thus, perpendicular to the polarization state of the leaked SPP-coupled light producing the image shown in Fig. 3(b).

III. CONCLUSIONS

We have demonstrated a plasmonic version of a quantum eraser. Using this technique, we were able to obtain an image

of the sample surface emission that reproduces with high fidelity the interference features existing at the metal-air interface. These interference features cannot be clearly observed in the images of the sample surface obtained without removing the which-path information carry on by the polarization state of the leakage radiation. We have demonstrated that in order to achieve the full potential of LRMs, one has to be able to manipulate the polarization state of the leaked light.

ACKNOWLEDGMENTS

This work was partially supported by the NSF CAREER Award No. ECCS-0954490, U.S. Army CERDEC Contract No. W15P7T-07-D-P040, and the J. F. Maddox Foundation.

¹M. O. Scully and K. Drühl, *Phys. Rev. A* **25**, 2208 (1982).

²T. J. Herzog, P. G. Kwiat, H. Weinfurter, and A. Zeilinger, *Phys. Rev. Lett.* **75**, 3034 (1995).

³S. P. Walborn, M. O. Terra Cunha, S. Pádua, and C. H. Monken, *Phys. Rev. A* **65**, 033818 (2002).

⁴W. Holladay, *Phys. Lett. A* **183**, 280 (1993).

⁵A. Drezet, A. Hohenau, D. Koller, A. Stepanov, H. Ditlbacher, B. Steinberger, F. R. Aussenegg, A. Leitner, and J. R. Krenn, *Mater. Sci. Eng., B* **149**, 220 (2008).

⁶J.-Y. Laluet, A. Drezet, C. Genet, and T. W. Ebbesen, *New J. Phys.* **10**, 105014 (2008).

⁷S. Massenot, J. Grandier, A. Bouhelier, G. Colas des Francs, L. Markey, J.-C. Weeber, A. Dereux, J. Renger, M. U. González, and R. Quidant, *Appl. Phys. Lett.* **91**, 243102 (2007).

⁸A. Drezet, A. Hohenau, A. L. Stepanov, H. Ditlbacher, B. Steinberger, N. Galler, F. R. Aussenegg, A. Leitner, and J. R. Krenn, *Appl. Phys. Lett.* **89**, 091117 (2006).

⁹D. W. Pohl, W. Denk, and M. Lanz, *Appl. Phys. Lett.* **44**, 651 (1984).

¹⁰S. P. Frisbie, C. Chesnutt, M. E. Holtz, A. Krishnan, L. Grave de Peralta, and A. A. Bernussi, *IEEE Photonics Journal* **1**, 153 (2009).

¹¹A. Krishnan, S. P. Frisbie, L. Grave de Peralta, and A. A. Bernussi, *Appl. Phys. Lett.* **96**, 111104 (2010).

¹²H. Raether, *Surface Plasmons on Smooth and Rough Surfaces and on Gratings* (Springer-Verlag, Berlin, 1988).

¹³G. Stabler, M. G. Somekh, and C. W. See, *J. Microsc.* **214**, 328 (2004).

¹⁴I. Gryczynski, J. Malicka, K. Nowaczyk, Z. Gryczynski, and J. R. Lakowicz, *J. Phys. Chem. B* **108**, 12073 (2004).

¹⁵S. P. Frisbie, C. J. Regan, A. Krishnan, C. Chesnutt, A. Ajimo, A. A. Bernussi, and L. Grave de Peralta, "Characterization of polarization states of surface plasmon polariton modes by Fourier-plane leakage microscopy," *Opt. Commun.* (2010).

¹⁶G. Zhu, M. Mayy, M. Bahoura, B. A. Ritzo, H. V. Gavrilenko, V. I. Gavrilenko, and M. A. Noginov, *Opt. Express* **16**, 15576 (2008).

¹⁷S. P. Frisbie, A. Krishnan, X. Xu, L. Grave de Peralta, S. A. Nikishin, M. W. Holtz, and A. A. Bernussi, *J. Lightwave Technol.* **27**, 2964 (2009).

¹⁸F. L. Pedrotti, L. S. Pedrotti, and L. M. Pedrotti, *Introduction to Optics*, 3rd ed. (Prentice-Hall, New Jersey, 2007).

¹⁹A. Kolomenski, A. Kolomenskii, J. Noel, S. Peng, and H. Schuessler, *Appl. Opt.* **48**, 5683 (2009).